Molecular Vision 2012; 18:2647-2657 <http://www.molvis.org/molvis/v18/a273>
Received 22 February 2011 | Accepted 27 October 2012 | Published 29 October 2012

Induction of amyloid-β_{1-42} in the retina and optic nerve head of chronic ocular hypertensive monkeys

Yasushi Ito,[1] Masamitsu Shimazawa,[1] Kazuhiro Tsuruma,[1] Chihiro Mayama,[2] Kiyoshi Ishii,[3] Hirotaka Onoe,[4] Makoto Aihara,[2] Makoto Araie,[5] Hideaki Hara[1]

(The first two authors contributed equally to this work.)

[1]Molecular Pharmacology, Department of Biofunctional Evaluation, Gifu Pharmaceutical University, Gifu, Japan; [2]Department of Ophthalmology, University of Tokyo Graduate School of Medicine, Tokyo, Japan; [3]Department of Ophthalmology, Saitama Red Cross Hospital, Saitama, Japan; [4]RIKEN Center for Molecular Imaging Science, Kobe, Japan; [5]Kanto Central Hospital, Tokyo, Japan

Purpose: Recent studies have indicated that accumulation of amyloid β_{1-42} ($A\beta_{1-42}$), which is associated with the progression of Alzheimer disease, may also be responsible for retinal ganglion cell death in glaucoma. The purpose of this study was to investigate the expression and localization of $A\beta_{1-42}$ in the retina and the optic nerve head (ONH) of monkeys with experimental glaucoma.

Methods: Five cynomolgus monkeys with a glaucomatous left eye at 4, 9, 11, 15, and 24 weeks after laser photocoagulation treatment were studied by immunohistochemical methods. Another two cynomolgus monkeys with a glaucomatous left eye at 133 weeks after laser photocoagulation treatment were used to measure $A\beta_{1-42}$ concentrations in the retina by enzyme-linked immunosorbent assay.

Results: At 11 to 24 weeks after the laser photocoagulation treatment, $A\beta_{1-42}$ was upregulated in the nerve fiber layer (NFL) and the ganglion cell layer (GCL) of the retina and the ONH, but the expression of amyloid precursor protein decreased in the NFL and ONH from levels at 9 weeks. The localizations of $A\beta_{1-42}$ were merged in glial fibrillary acidic protein-positive astroglial cells but not phosphorylated neurofilament heavy- or nonphosphorylated neurofilament heavy-positive axons in the retina and the ONH. Likewise, $A\beta_{1-42}$ concentrations in the retina of monkeys increased in the chronic stage of glaucoma.

Conclusions: These findings indicate that the upregulation of $A\beta_{1-42}$ after an intraocular pressure elevation could apply to monkeys since the structure of the ONH is more similar to humans than that of rodents.

Glaucoma is a multifactorial optic neuropathy characterized by retinal ganglion cell (RGC) death [1]. This irreversible RGC death results in progressive visual field loss along with decreased color sensitivity and contrast [2]. Although RGC death can be observed in patients with normal ocular tension [3], if genetic, environmental, and other factors are involved [4], elevated intraocular pressure (IOP) is a recognized risk factor for RGC degeneration in glaucoma. At present, the only well established treatment of glaucoma involves lowering the IOP; however visual field loss continues to progress in a subset of glaucoma patients even if medical and surgical treatments successfully lower the IOP [5]. Thus, new approaches to treating glaucoma, such as directly preventing RGC death, have been required in addition to regulating IOP.

Correspondence to: Hideaki Hara, Molecular Pharmacology, Department of Biofunctional Evaluation, Pharmaceutical University, 1-25-4 Daigaku-nishi, Gifu 501-1196, Japan; Phone: +81-58-230-8126; FAX: +81-58-230-8126; email: hidehara@gifu-pu.ac.jp.

Recent studies suggest that there is a significantly higher rate of glaucoma occurrence among patients with Alzheimer disease (AD), the most common form of dementia, than control subjects, suggesting a possible relationship between these two diseases [6,7]. AD is pathologically characterized by the extracellular accumulation of the amyloid β (Aβ) peptide in senile plaques within the brain [8]. Although the causal relationship between AD and Aβ still remains to be established, growing genetic and biochemical evidence strongly suggests that Aβ, especially the longer $A\beta_{1-42}$ isoform, plays a pivotal and early role in AD pathogenesis [9,10]. Interestingly, it has been reported that AD and glaucoma have many common features [4]. Sunderland et al. noted that levels of $A\beta_{1-42}$ significantly decreased in cerebrospinal fluid from AD patients in comparison with control subjects [11]. Subsequently, we reported that levels of $A\beta_{1-42}$ significantly decreased in the vitreous fluid from glaucoma patients in comparison with control subjects with macular hole [12]. On the other hand, a chronic elevation of IOP induces Aβ in RGCs in experimental rat glaucoma [4]. This result is consistent with some previous reports on experimental mouse

glaucoma models [13-15]. Furthermore, Guo et al. reported that neutralizing antibody to Aβ significantly delays and attenuates RGC apoptosis in experimental glaucoma [13]. These findings indicate that $A\beta_{1-42}$ neurotoxicity as AD brain may be involved in RGC death in glaucoma; however, the study by Guo and colleagues [13] did not use primate, but rodents (mouse and rat) for the study of experimental glaucoma. We consider an investigation by using monkeys to be important because the structure of the monkey optic nerve head (ONH) is more similar to humans than that of rodents. Hence, this is the first report that, by using experimental glaucoma monkeys, has shown the time-dependent expressions and localization of $A\beta_{1-42}$ in the retina as well as in the ONH after chronic IOP elevation.

METHODS

Animals: We used seven adult cynomolgus monkeys (*Macaca fascicularis*). Five monkeys aged 4–6 years (Nippon SLC, Hamamatsu, Japan) were used for immunohistochemistry. Another two monkeys was purchased from Shin Nippon Biomedical Laboratories, Ltd., (Tokyo, Japan). Two cynomolgus monkeys aged 4–5 years were used for enzyme-linked immunosorbent assay (ELISA). Each monkey was housed in an individual cage within a monkey colony. Ophthalmoscopic examinations conducted before the experiment revealed no ocular abnormalities in any of the monkeys. All experiments were performed in accordance with the Association for Research in Vision and Ophthalmology Statement for the Use of Animals in Ophthalmic and Vision Research and were approved and monitored by the Institutional Animal Care and Use Committee of the RIKEN Center for Molecular Imaging Science and the Institutional Animal Care and Use Committee of Tokyo University.

Induction of experimental glaucoma: Elevated IOP was induced by applying argon blue/green laser photocoagulation burns (Ultima 2000 SE®; Coherent Inc., Santa Clara, CA) to the trabecular meshwork of the left eye. The right eye was used as an untreated control, as previously described [16]. Briefly, the animals were anesthetized with an intramuscular injection of ketamine (8.75 mg/kg, Ketalar 50®; Sankyo, Tokyo, Japan) plus xylazine (0.5 mg/kg, Celactal®; Bayer, Leverkusen, Germany). A single-mirror Goldmann lens (OSMGA, Ocular Instruments, Inc., Bellevue, WA) filled with a hydroxyethylcellulose solution (Scopisol®15; Senjyu Pharmaceutical, Osaka, Japan) was then placed on the eye to be treated. An argon blue/green laser was focused on the mid-portion of the trabecular meshwork, and a total of 100 to 150 laser-beam spots was applied around 360° (spot size, 100 µm; power, 1000 mW; exposure time, 0.2 s) using an argon-laser photo-coagulator (Ultima 2000 SE®; Coherent, Inc., Santa Clara, CA) attached to a standard slit-lamp microscope (BQ 900; Haag-Streit, Köniz, Switzerland). IOP was measured in both eyes in each animal, using a calibrated pneumatonometer was used Model 30 Classic Pneumatonometer (Medtronic Solan, FL).

Histological analysis of the retina: After the final IOP measurement at 4 to 24 weeks after the first laser treatment, the monkeys were perfused via the common carotid artery with 0.9% saline containing 10 U/ml heparin at room temperature, followed by 4% paraformaldehyde in 0.01 M phosphate-buffered saline (PBS; 137 mM NaCl, 2.7 mM KCl, 10mM Na_2HPO_4, 1.8 mM KH_2PO_4, pH 7.4). This was done under deep general anesthesia (sodium pentobarbital 30 mg/kg, i.v). The eyes were removed after the perfusion. The eyes were immersed in the same fixative solution for at least 24 h, soaked in 10 to 30% (w/v) sucrose, and then frozen in embedding compound (Tissue-Tek; Sakura Finetechnical Co. Ltd., Tokyo, Japan). Next, 20-µm thick coronal sections of the retina were serially cut. Frozen sections (thickness, 20 µm) cut through the optic disc of each eye were used cryostat (Leica CM1850, Leica Microsystems Inc., Buffalo Grove, IL) and stained with hematoxylin and eosin.

During the immunofluorescent staining procedures for amyloid-β_{1-42} ($A\beta_{1-42}$), coronal sections of the retina were treated with 90% formic acid for 5 min for antigen retrieval. Coronal sections were then preincubated with 10% normal goat serum (Vector Laboratories, Burlingame, CA) in 0.01 M PBS for 30 min, then incubated for 1 day at 4 °C with specific rabbit anti-$A\beta_{1-42}$ polyclonal antibody (1:1,000 dilution; 171,609; Calbiochem, San Diego, CA) or anti-mouse anti-Alzheimer precursor protein monoclonal antibody (1:1,000 dilution; MAB348; Millipore, Temecula, CA), which recognizes all three isoforms of amyloid precursor protein (APP; immature, mature, and soluble APP [sAPP]), in a solution of 10% normal rabbit serum in 0.01 M PBS containing 0.3% (v/v) Triton X-100. Next, coronal sections incubated with each antibody were washed with 0.01 M PBS and then incubated for 3 h at room temperature with a mixture of an Alexa Fluor 488 $F(ab')_2$ fragment of goat anti-rabbit immunoglobulin G recognizing both heavy and light chains (IgG; H^+L; 1:1,000 dilution; A11070; Invitrogen, Carlsbad, CA) or an Alexa Fluor 488 $F(ab')_2$ fragment of rabbit anti-mouse IgG (H^+L; 1:1,000 dilution; A21204; Molecular Probes). At the end of immunostaining, Hoechst 33,342 (1:5,000 dilution) was added to the samples for 30 min to visualize the nuclei.

To visualize co-localization of $A\beta_{1-42}$ with glial fibrillary acidic protein (GFAP), phosphorylated neurofilament H (SMI-31) and nonphosphorylated neurofilament H (SMI-32)

double immunofluorescence was performed on sections of retina. Coronal sections of retina were washed with 0.01 M PBS and then treated with 90% formic acid for 5 min. Next, coronal sections were preincubated with 10% normal goat serum in 0.01 M PBS for 30 min, then incubated overnight at 4 °C with rabbit anti-$A\beta_{1-42}$ polyclonal antibody (1:1,000 dilution), mouse anti-GFAP monoclonal antibody (1:800 dilution; MAB360; Chemicon, Temecula, CA), mouse anti-SMI-31 monoclonal antibody (1:1,000 dilution; NE1022; Calbiochem), and mouse anti-SMI-32 monoclonal antibody (1:1,000 dilution; NE1023; Calbiochem) in a solution of 10% normal goat serum in 0.01 M PBS with 0.3% (v/v) Triton X-100. Next, coronal sections incubated with each antibody were washed with 0.01 M PBS and then incubated for 3 h at room temperature with a mixture of an Alexa Fluor 488 $F(ab')_2$ fragment of goat anti-rabbit IgG (H^+L; 1:1,000 dilution; A11070; Molecular Probes) and an Alexa Fluor 546 $F(ab')_2$ fragment of goat anti-mouse IgG (H^+L; 1:1,000 dilution; A-11018; Molecular Probes). At the end of immunostaining, Hoechst 33,342 (1:5,000 dilution) was added to the samples for 30 min to visualize the nuclei.

Images of the retina and ONH were taken using a microscope (BX50; Olympus, Tokyo, Japan) fitted with 4×, 20×, and 40× microscope objective lenses. The images visualized by hematoxylin and eosin stain (Figure 1) were taken using a charge-coupled device camera (MicroPublisher 5.0RTV; QIMAGING, Burnaby, Canada), and the cell counts in the ganglion cell layer (GCL) and inner nuclear layer (INL) at a distance between 1,750 and 2,200 µm from the optic disc toward the macula were measured on the images in a masked fashion by a single observer (Y. I.). Data from six sections were averaged for each eye, and the values obtained were used to evaluate the GCL cell counts. Immunofluorescence images (Figure 2 and Figure 3) were taken using a cooled charge-coupled device camera (DP30BP; Olympus) via Metamorph (Universal Imaging Corp., Downingtown, PA). The double immunofluorescence images (Figure 4 and Figure 5) were taken using a confocal microscope (FV10i; Olympus). The intensities of immunoreactivity in the retina and ONH were scored by a single observer who was blinded to the animals' data. Background immunoreactivity was represented with a minus sign (−). One plus (+) represented weak immunostaining intensity, two pluses (++) represented moderate immunostaining intensity, and three pluses (+++) represented robust immunostaining intensity (see Table 1).

Enzyme-linked immunosorbent assay of the retina: To measure soluble or insoluble $A\beta_{1-42,}$ monkey retinas were homogenized in tris-buffered saline (TBS) solution consisting of 50 mM Tris-HCl, pH 7.6, 150 mM NaCl, and protease inhibitors (P8340; Sigma-Aldrich, St. Louis, MO) and then centrifuged at 500,000 × *g* for 20 min at 4 °C. The pellets were dissolved in 200 µl of 1% Triton we dissolved in 1% Triton X-100/TBS/protease inhibitors and then homogenized. The homogenates were incubated for 15 min at 37 °C, and then centrifuged at 500,000 × *g* for 20 min. The supernatants were used as the Triton X-100 soluble fraction, while the pellets were dissolved in 200 µl of 2% sodium dodecyl sulfate (SDS)/TBS/protease inhibitors and then homogenized. The homogenates were incubated for 15 min at 37 °C and then centrifuged at 500,000 × *g* at 25 °C. Next, the pellets were dissolved in 70% formic acid and then ultrasonicated. Following centrifugation at 500,000 × *g* at 4 °C, the supernatants were collected and then dried by speed vacuum. Dried supernatants were dissolved in dimethyl sulfoxide and used as the Triton X-100 insoluble fraction. The concentration of $A\beta_{1-42}$ in the Triton X-100 soluble and insoluble fractions of the monkey retina was measured using the $A\beta_{1-42}$ ELISA Kit (292−64501; Wako, Osaka, Japan). ELISA for $A\beta_{1-42}$ was performed according to the manufacturer's protocol, and the monoclonal antibodies, BC05, contained in this kit specifically detects the C-terminal protein of $A\beta_{1-42}$. In this assay of standard solution and the sample solutions dispensed 100 µl into wells for 1 day at 4 °C. The monoclonal antibody, BC05, contained in this kit specifically detect the C-terminal protein of $A\beta_{1-42}$. Next, the wells were washed 3 times with wash solution, and then, dispensed 100 µl HRP-conjugated antibody solution into the wells for 1 h at 4 °C. Next, the wells were washed 3 times with wash solution, and then incubated for 30 min at room temperature with 100 µl TMB solution and then added 100 µl stop solution. The absorbance was measured at 450 nm using VARIOSKAN FLASH (Thermo Fisher Scientific, Waltham, MA). The absorbance was measured at 450 nm using VARIOSKAN FLASH (Thermo Fisher Scientific, Waltham, MA).

RESULTS

Retinal damage after intraocular pressure elevation: Although the nontreated right eyes did not display morphological changes in the retina and ONH, the glaucomatous eyes exhibited time-dependent changes (decreased cell number of the GCL and increased glaucomatous cup depth of the ONH) after IOP elevation (Figure 1 and Table 1). The mean cell number of the GCL was 839.3, 971.1, 360.7, 253.7, and 116.7 cells/mm in the laser-treated eyes, and 1076.7, 1097.3, 1007.0, 1058.9, and 1000.7 cells/mm in the fellow eyes of monkeys 1 to 5, respectively.

Expression and localization of amyloid β_{1-42} in the glaucomatous monkey eye: The IOP data and $A\beta_{1-42}$ immunoreactivites

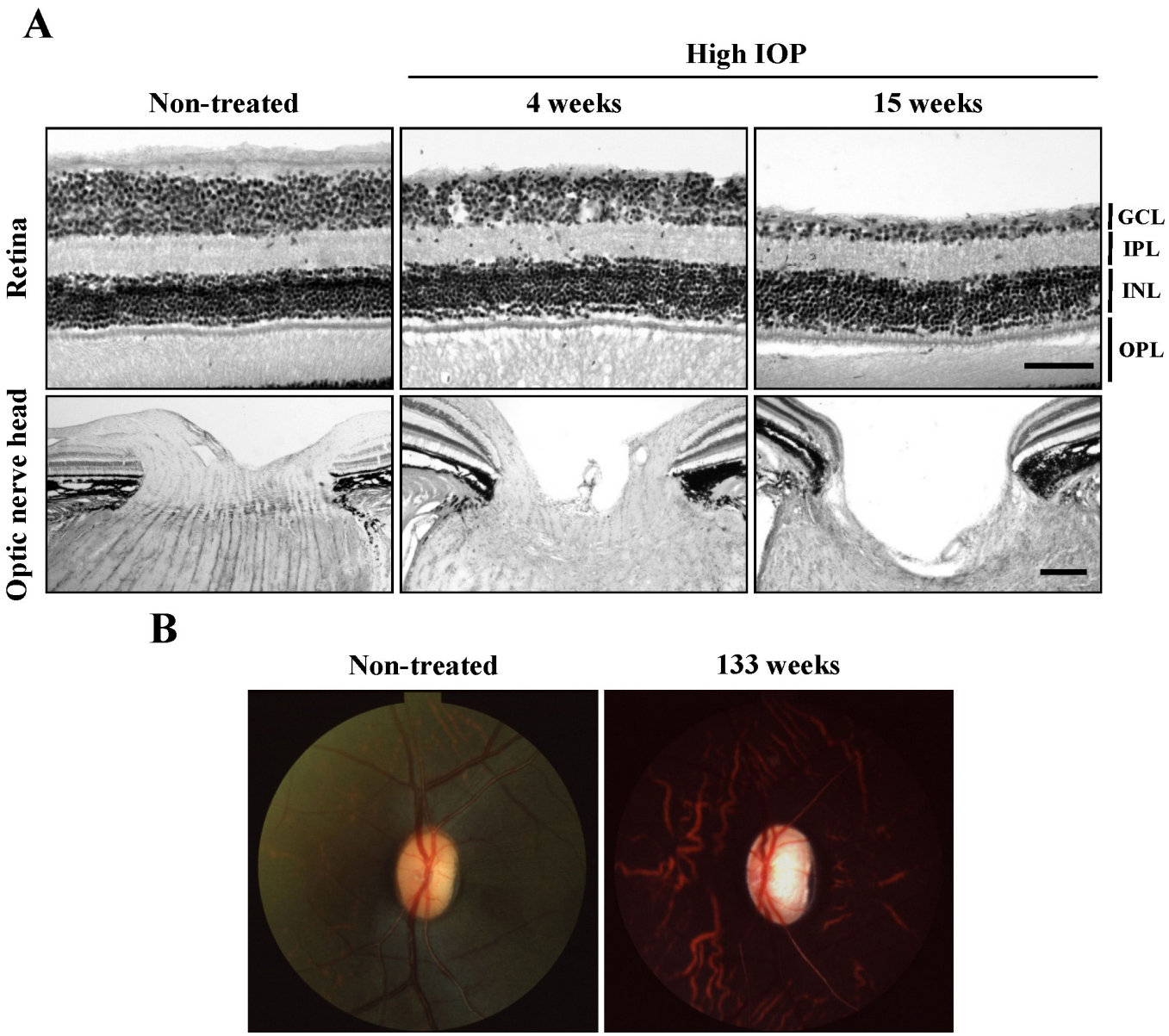

Figure 1. Morphological changes in retina and optic nerve head after chronic elevation of intraocular pressure. Representative photographs **A**: shows hematoxylin and eosin staining sections of retina and optic nerve head obtained from the eyes that had the pressure in their left eye elevated for 4 and 15 weeks and nontreated eye. Each scale bar indicates 100 µm for retina and 250 µm for ONH. Abbreviations are as follows: IOP represents intraocular pressure; GCL represents ganglion cell layer; IPL represents inner plexiform layer; INL represents inner nuclear layer; OPL represents outer plexiform layer. Fundus photographs in monkey. Representative fundus photographs showing nontreated eye, and treated eye at 133 weeks after IOP elevation **B**.

in the retina and ONH are summarized in Table 1. $A\beta_{1-42}$ immunoreactivity was present in the nerve fiber layer (NFL), GCL, and ONH of the monkey retina at 11, 15, and 24 weeks but not 4 or 9 weeks after the first laser treatment in this study (Figure 2). The $A\beta_{1-42}$ deposits (green) were detected overlying the NFL and/or surrounding cells in the GCL (Figure 2). On the other hand, there was a decrease in the APP expressions in the NFL and ONH at 9, 11, and 15 weeks after the first laser treatment (Figure 3).

Next, to identify the localization of $A\beta_{1-42}$-positive amyloid deposits, double immunofluorescence was performed for $A\beta_{1-42}$ and GFAP, SMI-31, or SMI-32 in the retina after IOP elevation. In the present study, $A\beta_{1-42}$ immunoreactivity was markedly increased in the monkey at 11 weeks after the first laser treatment (Figure 2, Table 1). We therefore used

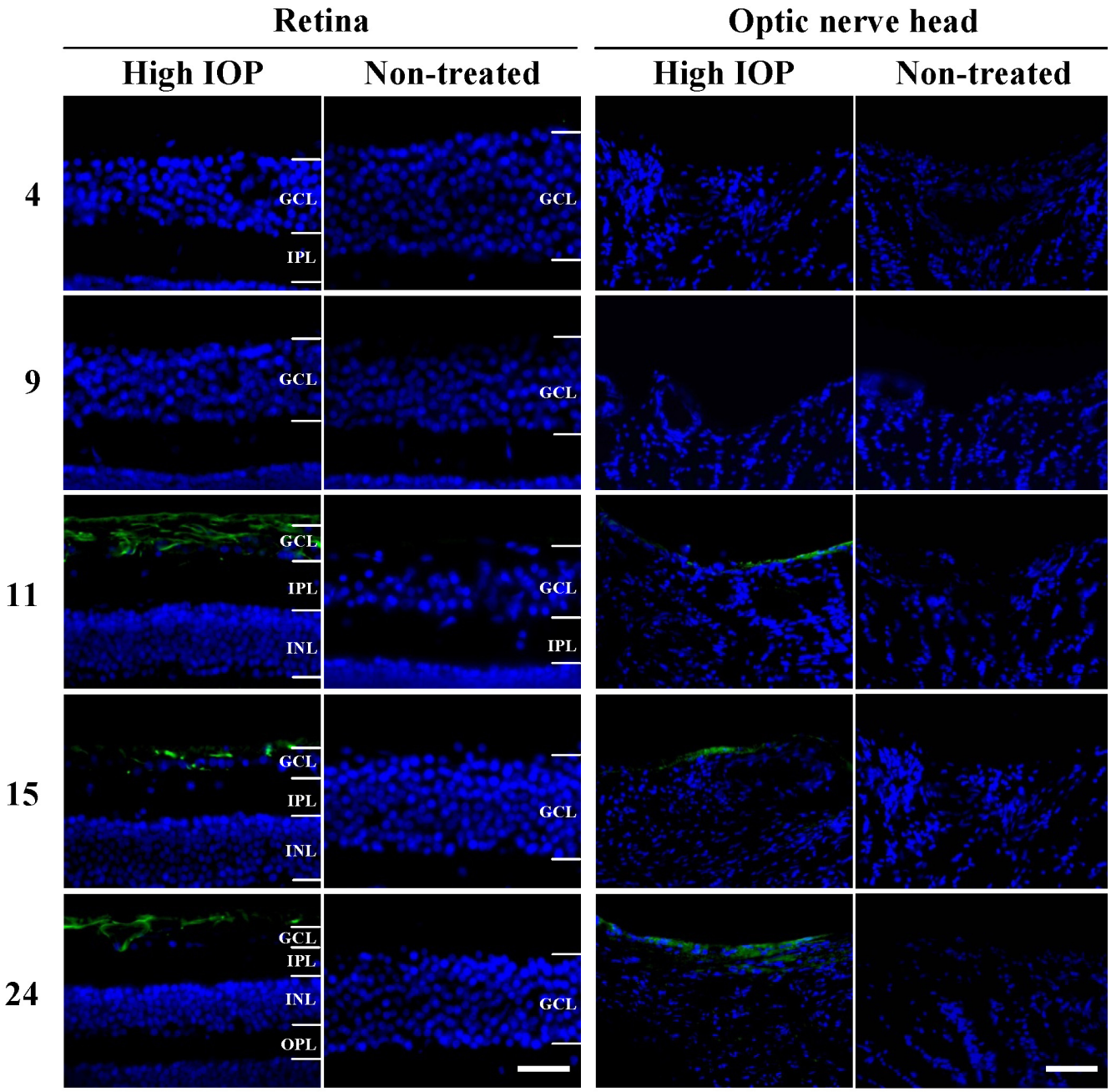

Figure 2. Time-dependent changes in the expression of amyloid β_{1-42} in retina and optic nerve head after laser photocoagulation treatment in cynomolgus monkeys. Representative photographs of retinal and optic nerve head (ONH) sections immunostained with anti-amyloid β ($A\beta_{1-42}$, green) and counterstained with Hoechst 33,342 (blue) were obtained from the monkeys that had the pressure in their left eye elevated at 4 to 24 weeks. $A\beta_{1-42}$ immunoreactivity was found to be increased in the nerve fiber layer (NFL), the ganglion cell layer (GCL), and ONH of the glaucomatous left eye from 11 weeks after IOP elevation, while there was no $A\beta_{1-42}$ immunoreactivity in the non-treated eye. Abbreviations are as follows: IOP represents intraocular pressure; IPL represents inner plexiform layer; INL represents inner nuclear layer; OPL represents outer plexiform layer. Horizontal scale bars indicate 50 μm.

the retinal section obtained from the monkey at 11 weeks after the first laser treatment. Figure 4 shows representative photographs of the retina double immunostained with $A\beta_{1-42}$ and GFAP, SMI-31, or SMI-32 at 11 weeks after IOP elevation. GFAP-positive astroglial cells in the NFL and the GCL of the retina but not SMI-31- or SMI-32-positive axons

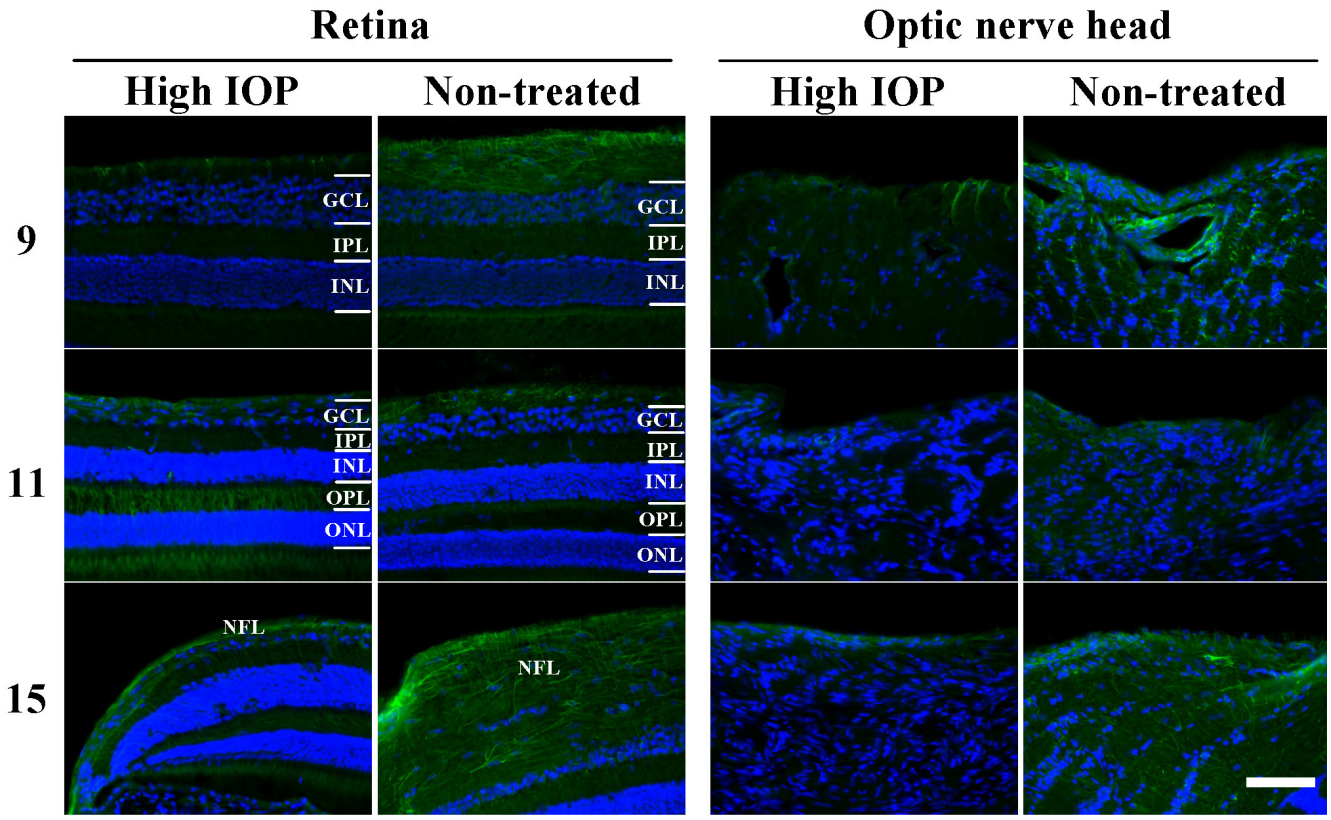

Figure 3. Time-dependent changes in the expression of amyloid procurer protein in retina and optic nerve head after laser photocoagulation treatment in cynomolgus monkeys. Representative photographs of retinal and optic nerve head (ONH) sections immunostained with anti- amyloid procurer protein (APP, green) and counterstained with Hoechst 33,342 (blue) were obtained from the monkeys that had the pressure in their left eye elevated at 9, 11, and 15 weeks. APP immunoreactivity was found to be decreased in retinal and ONH sections of the glaucomatous left eye from 9 weeks onward after intraocular pressure (IOP) elevation. Abbreviations are as follows: GCL represents ganglion cell layer; IPL represents inner plexiform layer; INL represents inner nuclear layer; OPL represents outer plexiform layer; ONL represents outer nuclear layer. Horizontal scale bar indicates 250 µm.

were found to express $A\beta_{1-42}$ at 11 weeks after the laser treatment. Concerning the localization of $A\beta_{1-42}$-positive amyloid deposits in the ONH, $A\beta_{1-42}$ was co-localized with GFAP-positive astroglial cells as well as $A\beta_{1-42}$ localization in the retina (Figure 5).

Concentrations of amyloid β_{1-42} in Triton X-100 insoluble and soluble fractions of retinal extracts: The concentrations of retinal tissue $A\beta_{1-42}$ as determined by ELISA are shown in Table 2. The Triton X-100 insoluble $A\beta_{1-42}$ concentrations in retinas were 1.41 and 0.76 pmol/mg protein in the glaucomatous left eye and nontreated right eye, respectively, of monkey 6, while those of monkey 7 were 4.56 and 0.81 pmol/mg protein, respectively. The Triton X-100 soluble $A\beta_{1-42}$ concentrations of the retina were 0.27 and 0.12 pmol/mg protein in the glaucomatous left eye and nontreated right eye, respectively, of monkey 6, while those of monkey 7 were 0.76 and 0.43 pmol/mg protein, respectively. Compared with the nontreated right eye, the Triton X-100 insoluble and soluble $A\beta_{1-42}$ concentrations of the retina increased in the glaucomatous left eye in both monkeys 6 and 7.

DISCUSSION

In the present study we observed the expression and localization of $A\beta_{1-42}$ in the retina and the ONH of monkeys with experimental glaucoma by using immunohistochemistry and ELISA. Advanced stage of RGC death and glaucomatous cupping in the ONH were observed to be time dependent at 11, 15, and 24 weeks after chronic IOP elevation.

APP is processed through non-amyloidogenic or amyloidogenic pathways. In the non-amyloidogenic pathway, α-secretase cleaves APP within the Aβ domain, thus preventing Aβ generation [17-20]. In contrast, APP cleaved

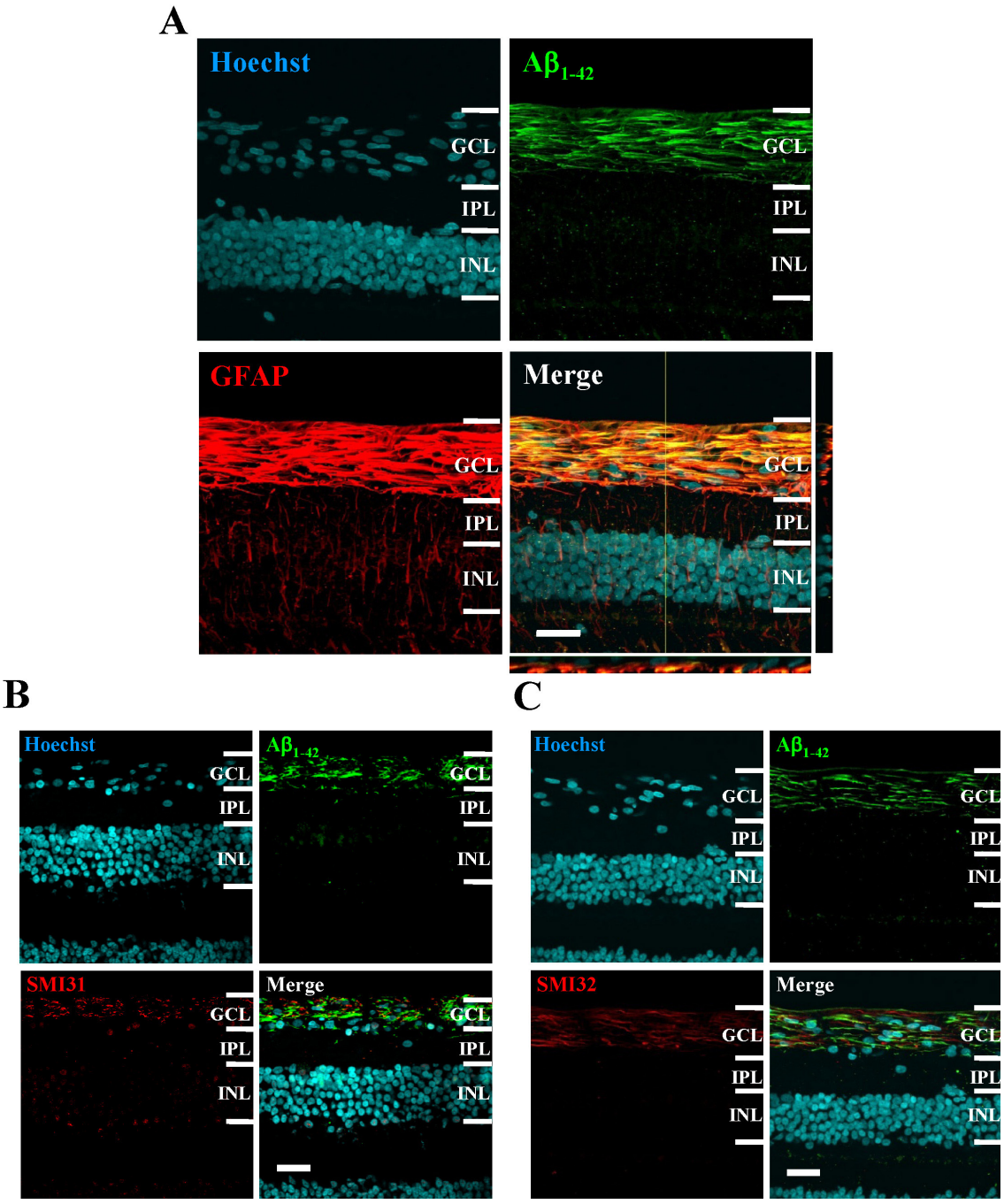

Figure 4. Representative photographs show amyloid β_{1-42} ($A\beta_{1-42}$)/glial fibrillary acidic protein (GFAP; **A**), $A\beta_{1-42}$/phosphorylated neurofilament H (SMI-31; **B**) and $A\beta_{1-42}$/non-phosphorylated neurofilament H (SMI-32; **C**) immunofluorescence stainings from monkey retina at 11 weeks after the laser photocoagulation treatment. $A\beta_{1-42}$ was colocalized with GFAP, but not SMI-31- or SMI-32, in the nerve fiber layer (NFL) and the ganglion cell layer (GCL) of the retina at 11 weeks after the laser photocoagulation treatment. Abbreviations are as follows: Hoechst represents Hoechst33342; IPL represents inner plexiform layer; INL represents inner nuclear layer. Horizontal scale bars indicate 30 μm.

by β- and γ-secretases produces Aβ, which may aggregate, deposit, and form ion channels in the cell plasma membrane, leading to neuronal death [17-21]. In the present study, APP expressions decreased in the NFL and ONH from 9 weeks after IOP elevation. APP might therefore be expected to decrease at a rate equal to the increased accumulation of Aβ

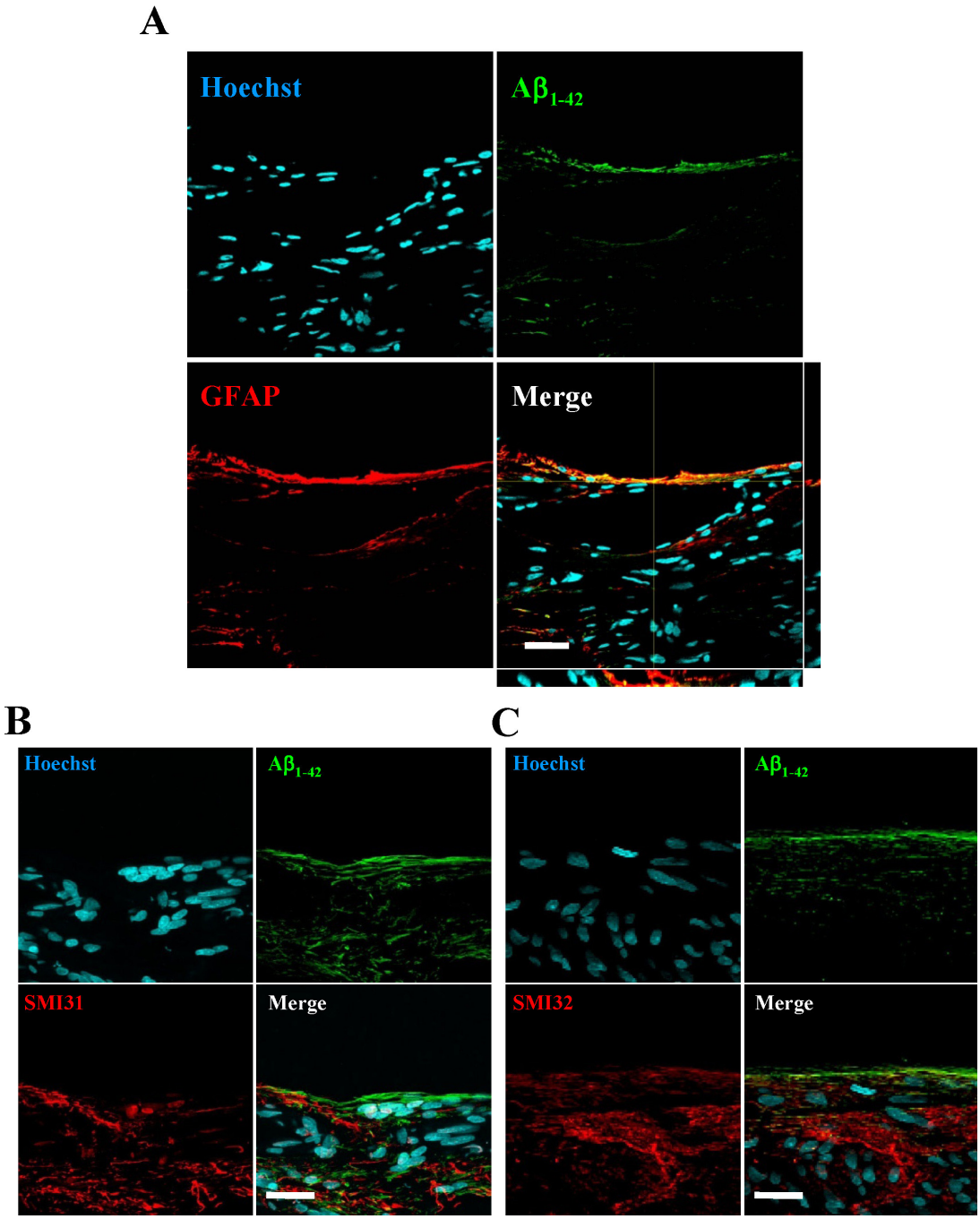

Figure 5. Immunolocalizations of amyloid β_{1-4} ($A\beta_{1-42}$) in the optic nerve head of cynomolgus monkeys. Representative photographs showing of amyloid β_{1-4} ($A\beta_{1-42}$)/glial fibrillary acidic protein (GFAP: **A**). $A\beta_{1-42}$/phosphorylated neurofilament H (SMI-31: **B**) and $A\beta_{1-42}$/non-phosphorylated neurofilament H (SMI-32: **C**) immunofluorescence stainings from monkey optic nerve head (ONH) at 11 weeks after laser photocoagulation treatment. $A\beta_{1-42}$ was co-localized with GFAP but not SMI-31 or SMI-32 in the ONH at 11 weeks after laser photocoagulation treatment. Horizontal scale bars indicate 30 µm.

[17,18]. In addition, RGC loss after chronic IOP elevation was consistent with the increased expression of $A\beta_{1-42}$ in the retina and ONH. These findings indicate that an increase in expressions of $A\beta_{1-42}$ may play a role in the progressive degeneration of RGCs and their axons that is usually associated with elevated IOP in primates and rodents [3,13,14]. Likewise, concentrations of $A\beta_{1-42}$ in the retina increased in the chronic stage (at 133 weeks after chronic IOP elevation) of glaucoma

Table 1. Changes in intraocular pressure (IOP) and $Ab_{1–42}$ immunoreactivity after laser photocoagulation treatment of the left eye in cynomolgus monkeys.

Animal number	Duration (weeks)	Mean IOP (mm Hg)		Grades of Aβ1–42 immunoreactivity	
				Retina	ONH
1	4	Left	48.7	−	−
		Right	26.2	−	−
2	9	Left	40	−	−
		Right	23.2	−	−
3	11	Left	60.2	+++	+
		Right	23.2	−	−
4	15	Left	62.1	++	+
		Right	26.8	−	−
5	24	Left	49	++	+
		Right	25.5	−	−

This table identifies the duration of laser photocoagulation treatment, mean IOP, and $Aβ_{1–42}$ immunoreactivities in the retina and optic nerve head (ONH) after laser photocoagulation treatment. The left eye was treated with laser photocoagulation and the right eye was used as a non-treated control in each monkey. Abbreviations: tissue not stained (−),weak immunostaining intensity (+), moderate immunostaining intensity (++), and robust immunostaining intensity (+++). The grading was performed by a single observer who was blinded to the animals' data.

in monkeys (Table 2). However, increased expressions of $Aβ_{1–42}$ were not found in the retina and ONH of the monkeys at the early phase (4 and 9 weeks) after IOP elevation (Figure 2). Thus, we were able to observe increased expressions of $Aβ_{1–42}$, consistent with RGC loss and glaucomatous cupping in monkeys, even with the small sample sizes of our study.

The expression of $Aβ_{1–42}$ in GFAP-positive astroglial cells was upregulated in the NFL and the GCL of the retina as well as in the ONH in experimental glaucoma in monkey eyes. The presence of large numbers of astroglial cells associated with $Aβ_{1–42}$ in the retina and the ONH suggests that these lesions may generate chemotactic molecules that mediate astroglial cell recruitment after chronic IOP elevation [22-24]. In fact, recruited astroglial cells assemble at the Aβ, most likely prolonging neuroinflammation [24]. Furthermore, retinal abnormalities, such as an increase in astrocyte glial cells, atrophy of the NFL, and loss of cells in the GCL, have been observed in AD patients [25-27], and accumulation of Aβ in the retina of the 27-month AD mice model promoted the overexpression of monocyte chemotactic protein-1 by cells in the GCL, leading to loss of cells in the GCL [28]. Therefore, the role of $Aβ_{1–42}$ co-localized with astroglial cells may not be beneficial under certain conditions related to chronic stress.

On the other hand, astroglial cells are important for $Aβ_{1–42}$ degradation and clearance. In this processes, astroglial cells detect $Aβ_{1–42}$ deposits and then cover them. Subsequently, $Aβ_{1–42}$ is incorporated into the astroglial cells, which degrade the $Aβ_{1–42}$ [22,23]. In fact, our previous study indicated that

Table 2. Ab1–42 concentrations of retina in the chronic stage of a glaucomatous left eye.

Animal number	Duration (weeks)	Mean IOP (mm Hg)		AB1–42 (pmol/mg protein)	
				Triton X-100	
				Insoluble fraction	Soluble fraction
6	133	Left	30.4	1.41	0.27
		Right	18.8	0.76	0.12
7	133	Left	29.5	4.56	0.76
		Right	19.6	0.81	0.43

This table identifies duration of laser photocoagulation treatment, mean intraocular pressure (IOP), and concentrations of $Aβ_{1–42}$ in Triton X-100 insoluble and soluble fraction of retina after the laser photocoagulation treatment. The left eye was treated with the laser photocoagulation and the right eye was used as a non-treated control in each monkey. The concentrations of retinal tissue $Aβ_{1–42}$ were measured by ELISA.

the activity of neprilysin, a zinc-dependent metalloprotease involved in the physiologic degradation of $A\beta_{1-42}$, and Aβ concentrations in vitreous fluid displayed converse changes in patients with proliferative diabetic retinopathy (compared to patients with macular hole), with a significant inverse correlation between the two parameters [29]. We also found that concentrations of $A\beta_{1-42}$ significantly decrease in the vitreous fluid of glaucoma patients (compared to macular hole patients) [12]; however, we did not investigate neprilysin activity and $A\beta_{1-42}$ concentrations in vitreous fluid obtained from monkeys with experimental glaucoma in this study. Furthermore, $A\beta_{1-42}$ in the retina appears to be eliminated by the action of metalloproteases, which are localized in astroglial cells closely associated with the accumulation of $A\beta_{1-42}$ [30,31]. These findings suggest that astroglial cells possess the requisite elements for $A\beta_{1-42}$ degradation. However, we could not conclude from our data to clarify it, and therefore further experiments will be needed to clarify the precise mechanisms.

In conclusion, the present study has provided novel information concerning the time-dependent expressions and localization of $A\beta_{1-42}$ in the retina and ONH in monkeys after chronic IOP elevation. These findings indicate that the upregulation of $A\beta_{1-42}$ after an IOP elevation applies to monkeys as well as rodents. Therefore, the modulation of $A\beta_{1-42}$ potential target for therapeutic interventions against glaucoma.

ACKNOWLEDGMENTS

This study was supported in part by Grants-in-Aid for Scientific Research (B; No. 22,390,321) and (C; Nos. 20,592,082 and 21,592,262) from the Ministry of Education, Culture, Sports, Science, and Technology, Japan, by Grant-in-Aid for Japan Society for the Promotion of Science (No. 20·10786), by Takeda Science Foundation, and by consignment expenses from the Molecular Imaging Program on the ‘‘Research Base for Exploring New Drugs’’ [Ministry of Education, Culture, Sports, Science and Technology (MEXT), Japan].

REFERENCES

1. Quigley HA, Broman AT. The number of people with glaucoma worldwide in 2010 and 2020. Br J Ophthalmol 2006; 90:262-7. [PMID: 16488940].
2. Mozaffarieh M, Grieshaber MC, Flammer J. Oxygen and blood flow: players in the pathogenesis of glaucoma. Mol Vis 2008; 14:224-33. [PMID: 18334938].
3. Tomita G. The optic nerve head in normal-tension glaucoma. Curr Opin Ophthalmol 2000; 11:116-20. [PMID: 10848217].
4. McKinnon SJ, Lehman DM, Kerrigan-Baumrind LA, Merges CA, Pease ME, Kerrigan DF, Ransom NL, Tahzib NG, Reitsamer HA, Levkovitch-Verbin H, Quigley HA, Zack DJ. Caspase activation and amyloid precursor protein cleavage in rat ocular hypertension. Invest Ophthalmol Vis Sci 2002; 43:1077-87. [PMID: 11923249].
5. The effectiveness of intraocular pressure reduction in the treatment of normal-tension glaucoma. Collaborative Normal-Tension Glaucoma Study Group. Am J Ophthalmol 1998; 126:498-505. [PMID: 9780094].
6. Bayer AU, Ferrari F, Erb C. High occurrence rate of glaucoma among patients with Alzheimer’s disease. Eur Neurol 2002; 47:165-8. [PMID: 11914555].
7. Bayer AU, Keller ON, Ferrari F, Maag KP. Association of glaucoma with neurodegenerative diseases with apoptotic cell death: Alzheimer’s disease and Parkinson’s disease. Am J Ophthalmol 2002; 133:135-7. [PMID: 11755850].
8. Pepys MB. Amyloidosis. Annu Rev Med 2006; 57:223-41. [PMID: 16409147].
9. Blennow K, de Leon MJ, Zetterberg H. Alzheimer’s disease. Lancet 2006; 368:387-403. [PMID: 16876668].
10. Andreasson U, Portelius E, Andersson ME, Blennow K, Zetterberg H. Aspects of beta-amyloid as a biomarker for Alzheimer’s disease. Biomark Med 2007; 1:59-78. [PMID: 20477461].
11. Sunderland T, Linker G, Mirza N, Putnam KT, Friedman DL, Kimmel LH, Bergeson J, Manetti GJ, Zimmermann M, Tang B, Bartko JJ, Cohen RM. Decreased β-amyloid1–42 and increased tau levels in cerebrospinal fluid of patients with Alzheimer disease. JAMA 2003; 289:2094-103. [PMID: 12709467].
12. Yoneda S, Hara H, Hirata A, Fukushima M, Inomata Y, Tanihara H. Vitreous fluid levels of β-amyloid$_{1-42}$ and tau in patients with retinal diseases. Jpn J Ophthalmol 2005; 49:106-8. [PMID: 15838725].
13. Guo L, Salt TE, Luong V, Wood N, Cheung W, Maass A, Ferrari G, Russo-Marie F, Sillito AM, Cheetham ME, Moss SE, Fitzke FW, Cordeiro MF. Targeting amyloid-β in glaucoma treatment. Proc Natl Acad Sci USA 2007; 104:13444-9. [PMID: 17684098].
14. Goldblum D, Kipfer-Kauer A, Sarra GM, Wolf S, Frueh BE. Distribution of amyloid precursor protein and amyloid-β immunoreactivity in DBA/2J glaucomatous mouse retinas. Invest Ophthalmol Vis Sci 2007; 48:5085-90. [PMID: 17962460].
15. Shimazawa M, Inokuchi Y, Okuno T, Nakajima Y, Sakaguchi G, Kato A, Oku H, Sugiyama T, Kudo T, Ikeda T, Takeda M, Hara H. Reduced retinal function in amyloid precursor protein-over-expressing transgenic mice *via* attenuating glutamate-*N*-methyl-D-aspartate receptor signaling. J Neurochem 2008; 107:279-90. [PMID: 18691390].
16. Quigley HA, Hohman RM. Laser energy levels for trabecular meshwork damage in the primate eye. Invest Ophthalmol Vis Sci 1983; 24:1305-7. [PMID: 6885314].

17. Guo L, Duggan J, Cordeiro MF. Alzheimer's disease and retinal neurodegeneration. Curr Alzheimer Res 2010; 7:3-14. [PMID: 20205667].

18. Surguchev A, Surguchov A. Conformational diseases: looking into the eyes. Brain Res Bull 2010; 81:12-24. [PMID: 19808079].

19. Tatton W, Chen D, Chalmers-Redman R, Wheeler L, Nixon R, Tatton N. Hypothesis for a common basis for neuroprotection in glaucoma and Alzheimer's disease: anti-apoptosis by alpha-2-adrenergic receptor activation. Surv Ophthalmol 2003; 48:Suppl 1S25-37. [PMID: 12852432].

20. Vickers JC. The cellular mechanism underlying neuronal degeneration in glaucoma: parallels with Alzheimer's disease. Aust N Z J Ophthalmol 1997; 25:105-9. [PMID: 9267595].

21. Ramkumar HL, Zhang J, Chan CC. Retinal ultrastructure of murine models of dry age-related macular degeneration (AMD). Prog Retin Eye Res 2010; 29:169-90. [PMID: 20206286].

22. Nagele RG, D'Andrea MR, Lee H, Venkataraman V, Wang HY. Astrocytes accumulate Aβ42 and give rise to astrocytic amyloid plaques in Alzheimer disease brains. Brain Res 2003; 971:197-209. [PMID: 12706236].

23. Nagele RG, Wegiel J, Venkataraman V, Imaki H, Wang KC. Contribution of glial cells to the development of amyloid plaques in Alzheimer's disease. Neurobiol Aging 2004; 25:663-74. [PMID: 15172746].

24. Sastre M, Klockgether T, Heneka MT. Contribution of inflammatory processes to Alzheimer's disease: molecular mechanisms. Int J Dev Neurosci 2006; 24:167-76. [PMID: 16472958].

25. Hinton DR, Sadun AA, Blanks JC, Miller CA. Optic-nerve degeneration in Alzheimer's disease. N Engl J Med 1986; 315:485-7. [PMID: 3736630].

26. Blanks JC, Torigoe Y, Hinton DR, Blanks RH. Retinal pathology in Alzheimer's disease. I. Ganglion cell loss in foveal/parafoveal retina. Neurobiol Aging 1996; 17:377-84. [PMID: 8725899].

27. Blanks JC, Schmidt SY, Torigoe Y, Porrello KV, Hinton DR, Blanks RH. Retinal pathology in Alzheimer's disease. II. Regional neuron loss and glial changes in GCL. Neurobiol Aging 1996; 17:385-95. [PMID: 8725900].

28. Ning A, Cui J, To E, Ashe KH, Matsubara J. Amyloid-beta deposits lead to retinal degeneration in a mouse model of Alzheimer disease. Invest Ophthalmol Vis Sci 2008; 49:5136-43. [PMID: 18566467].

29. Hara H, Oh-hashi K, Yoneda S, Shimazawa M, Inatani M, Tanihara H, Kiuchi K. Elevated neprilysin activity in vitreous of patients with proliferative diabetic retinopathy. Mol Vis 2006; 12:977-82. [PMID: 16943769].

30. Iwata N, Tsubuki S, Takaki Y, Watanabe K, Sekiguchi M, Hosoki E, Kawashima-Morishima M, Lee HJ, Hama E, Sekine-Aizawa Y, Saido TC. Identification of the major $A\beta_{1-42}$-degrading catabolic pathway in brain parenchyma: suppression leads to biochemical and pathological deposition. Nat Med 2000; 6:143-50. [PMID: 10655101].

31. Apelt J, Ach K, Schliebs R. Aging-related down-regulation of neprilysin, a putative β-amyloid-degrading enzyme, in transgenic Tg2576 Alzheimer-like mouse brain is accompanied by an astroglial upregulation in the vicinity of β-amyloid plaques. Neurosci Lett 2003; 339:183-6. [PMID: 12633883].

Articles are provided courtesy of Emory University and the Zhongshan Ophthalmic Center, Sun Yat-sen University, P.R. China. The print version of this article was created on 29 October 2012. This reflects all typographical corrections and errata to the article through that date. Details of any changes may be found in the online version of the article.